The Relationship between Drop In-Cloud Residence Time and Drizzle Production in Numerically Simulated Stratocumulus Clouds

GRAHAM FEINGOLD,* BJORN STEVENS,† W. R. COTTON,* AND A. S. FRISCH†

*Cooperative Institute for Research in the Atmosphere, Colorado State University, Fort Collins, Colorado
†Department of Atmospheric Science, Colorado State University, Fort Collins, Colorado

(Manuscript received 10 May 1995, in final form 3 October 1995)

ABSTRACT

This paper considers the production of drizzle in stratocumulus clouds in relation to the boundary-layer turbulent kinetic energy and in-cloud residence times. It is shown that drizzle production in stratocumulus of the order of 400 m in depth is intimately related to the vertical velocity structure of the cloud eddies. In a series of two-dimensional numerical experiments with fixed cloud condensation nucleus concentrations, the effect on drizzle production of enhanced or diminished vertical velocities is simulated. Rather than do this by simulating clouds exhibiting more or less energy, we modify drop terminal velocities in a manner that conserves the fall velocity relative to the air motions and allows droplet growth to occur in a similar dynamical environment. The results suggest that more vigorous clouds produce more drizzle because they enable longer in-cloud dwell times and therefore prolonged collision–coalescence. In weaker clouds, droplets tend to fall out of the cloud before they have achieved significant size, resulting in smaller amounts of drizzle. In another series of experiments, we investigate the effects of the feedback of drizzle on the boundary-layer dynamics. Results show that when significant amounts of drizzle reach the surface, the subcloud layer is stabilized, circulations are weaker, and the boundary layer is not well mixed. When only small amounts of drizzle are produced, cooling tends to be confined to the region just below cloud base, resulting in destabilization, more vigorous circulations, and a better mixed boundary layer. The results strongly suggest that a characteristic time associated with collision–coalescence be incorporated into drizzle parameterizations.

1. Introduction

Although stratocumulus clouds are not prodigious producers of precipitation, the small amounts of drizzle they do produce has an important impact on both cloud *macro*physical properties (e.g., spatial coverage, depth and liquid water content) and *micro*physical properties (e.g., droplet size distributions, effective radii). The radiative effects of stratocumulus are intimately connected to both these macro- and microphysical properties, and it is thus essential that we understand the drizzle production mechanism if our predictions of climate forcing by these clouds is to have a sound basis.

Over the past decades, stratocumulus cloud studies have focused on a number of primary issues. These have included (but are not limited to) cloud-top entrainment instability (Lilly 1968; Randall 1980; Deardorff 1980), maintenance of a steady cloud depth against the effects of subsidence (e.g., Roach et al. 1982; Moeng 1986), and cloud-top radiative cooling (e.g., Oliver et al. 1978). Two main classes of models have been applied to the problem of a classical well-mixed boundary layer: layer-averaged models (including entity-type models, higher-order closure models, and two-layer models), and large eddy simulation (LES) models. Field programs such as FIRE-Stratocumulus (Cox et al. 1987) have contributed greatly to our understanding of this prevalent cloud type. Although there exists in the literature both observational evidence (e.g., Brost et al. 1982; Nicholls 1984) and modeling studies (e.g., Chen and Cotton 1987; Nicholls 1987; Pincus and Baker 1994; Austin et al. 1995) of drizzle, precipitating stratocumulus clouds have not received the same degree of scrutiny as their nonprecipitating counterparts. Certainly within the realm of modeling studies, it is only recently that LES models coupled to explicit microphysical models have come to the fore (Kogan et al. 1994, 1995; Feingold et al. 1994a; Stevens et al. 1996), but to date they have not been applied specifically to the drizzle problem. This absence is noteworthy since the latter class of model represents the most appropriate framework for modeling of the drizzle process, in that it explicitly solves for the growth of a size-spectrum of drops and resolves most of the turbulent energy of the eddies supporting these drops. The prevalence of drizzle during the ASTEX (Atlantic Stratocumulus Transition Experiment 1992) has provided a rich dataset from both in situ measurements (e.g., Martin et al. 1995) and remote sensors (Frisch et al. 1995), and there is increased in-

Corresponding author address: Dr. Graham Feingold, CIRA/NOAA, 325 Broadway, Boulder, Co. 80303.

terest in the impact that these small amounts of precipitation have on the structure of the boundary layer.

A major question that needs to be resolved relates to the mechanisms of droplet growth that generate precipitation-sized droplets. Albrecht (1989) perceived drizzle to be related to cloud condensation nucleus (CCN) number and size. The hypothesis is that enhanced concentrations of CCN will generate higher concentrations of cloud droplets. Condensational growth is then limited by competition for available vapor, and unless droplets above some critical size are formed, the collision–coalescence mechanism and, consequently, the formation of drizzle will be suppressed. Frequently, a source of giant CCN (size > 1 μm) is suggested as a means to stimulate the gravitational collection mechanism (e.g., Johnson 1982) by establishing a large enough dispersion of drop sizes. Other studies have stressed dynamic and thermodynamic considerations, and the relationship between drizzle and large-scale convective forcing (e.g., Paluch and Lenschow 1991) has been examined. In this regard, two-layer models (e.g., Albrecht 1993) and mixed-layer models (e.g., Pincus and Baker 1994) have been used to simulate drizzle formation by parameterizing the process in terms of macroscale parameters such as cloud depth and assumed values of droplet size or concentration. Models of this type do not resolve the structure of the boundary-layer (BL) eddies due to their assumption of horizontal homogeneity.

Cloud dynamics are well known to drive cloud microphysics; for example, the local updraft velocity determines supersaturation production and the number of activated droplets. Microphysical processes also affect the dynamics; for nondrizzling clouds, this may occur if cloud-top cooling—a primary driving force of the circulations—is affected by shortwave radiation, which is dependent on droplet size (Slingo 1989). For drizzling clouds, the impact of microphysics on dynamics is primarily due to the vertical redistribution of heat and vapor. This can manifest itself in different ways; modification of cloud water lost to drizzle will affect cloud-top cooling; removal of cloud water will result in a net heating of the cloud layer; evaporation of precipitation below cloud base will affect the stability of the subcloud layer.

Thus, for both in-cloud and drizzle processes, it is important to model both dynamics and microphysics in as realistic a manner as possible. To do so, a number of models, including a three-dimensional large eddy simulation (LES) model and its two-dimensional version (usually termed a cloud resolving model, or CRM) have been adapted to include explicit (size-resolving) microphysical treatment of the CCN and droplet spectra (Feingold et al. 1994a; Stevens et al. 1996). By directly calculating processes such as droplet growth by condensation and stochastic collection, evaporation, and sedimentation in the LES or CRM framework, a position is established to better represent cloud microphysics and dynamics and to elucidate the drizzle-formation process. Most other finite-difference modeling studies of precipitating stratocumulus in two or three dimensions [with the exception of Kogan et al. (1994, 1995)] employ bulk microphysical formulations of microphysics where the growth of precipitation-sized drops is parameterized through an autoconversion process. These models typically assign one average fall velocity to all of the precipitation-sized drops. In nonprecipitating stratocumulus, these limitations are not severe, but for the current study, it is important to perform accurate calculations of (a) droplet growth through collection, and (b) the differential (size-dependent) fall velocities associated with each drop size bin. Perhaps the greatest advantage of the explicit microphysical formulation in stratocumulus studies is that it accurately represents these two processes. The collision–coalescence process is represented by the quasi-stochastic equation, and each drop size bin is assigned its appropriate terminal fall velocity. Thus, precipitation is spread in the vertical in a more natural manner, and the modification of the profiles of heat and vapor due to condensation–evaporation are better predicted.

This paper will attempt to elucidate only one aspect of drizzle formation, namely, the relationship between it and a measure of the kinetic energy of the cloud (in this case root-mean-square velocity $w_{\rm rms}$) and, by association, drop in-cloud residence times. For boundary layers driven primarily by buoyancy, $w_{\rm rms}^2$ is of similar order of magnitude to turbulent kinetic energy (TKE).

It is noted at this point that TKE impacts drop collection in ways other than to increase in-cloud residence times. For example, a number of studies have suggested that drop-collection efficiencies increase with increasing TKE due to a drop-size-dependent response to the turbulence (e.g., de Almeida 1976; Khain 1995) or by creating an overlap of spatially separated eddies (Reuter et al. 1988). At present the magnitude of these effects is not well established. This paper does not consider the impact of TKE on collection efficiencies. TKE also affects cloud-top entrainment, which too may promote drizzle formation (e.g., Telford and Wagner 1981). Although cloud-top entrainment is represented by the model and simulated entrainment velocities appear reasonable, the relationship between entrainment and drizzle formation has not been directly addressed here. Thus, throughout this work, the effect of TKE is equated with its effect on drop in-cloud residence times.

The authors follow the classic work of Bowen (1950) and Mason (1952), who calculated the growth of a large collector droplet rising in an updraft while collecting small droplets. The large drop continues to rise until its terminal velocity exceeds the updraft velocity, at which point it begins to fall through the cloud. Bowen showed that the size of the drop as it exits the cloud depends on the updraft velocity and cloud liquid water content, (LWC). Ma-

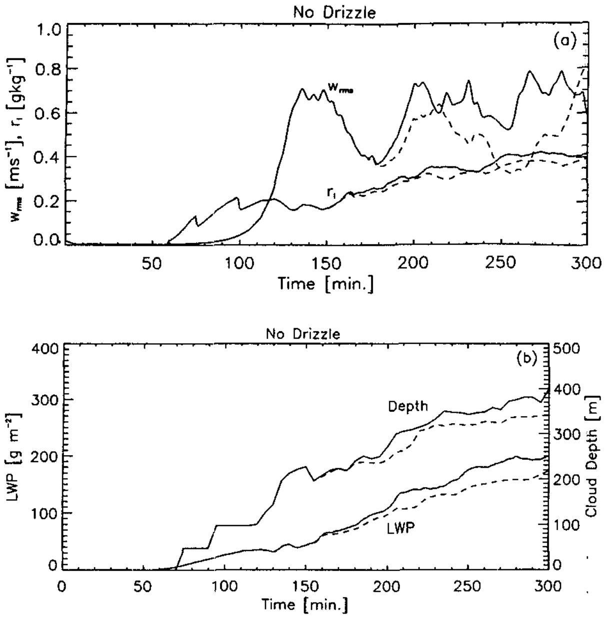

FIG. 1. Temporal evolution of (a) w_{rms} and r_l and (b) LWP and cloud depth for the nonprecipitating case. The solid line represents stronger longwave forcing, while the dashed line represents weaker longwave forcing.

son argued that the turbulent motions in stratiform clouds will allow drizzle drops to form by increasing their dwell time in the cloud. Nicholls (1987) followed this line of thought by studying stochastic drop coalescence within a stochastic turbulence model. His ideas have been developed further by Baker (1993) and Austin et al. (1995). Here the authors will use a rather more sophisticated model but build on the ideas of Bowen, Mason, and Nicholls.

This work differs from the aforementioned works in a number of respects. First, droplet growth processes are explicitly modeled, as are the mechanisms through which some statistically fortunate droplets grow large enough to initiate gravitational collection. Second, given the fact that these droplets do exist, an examination is made of how important the turbulent motion is within the cloud in determining the amount of precipitation produced. Third, the impact of precipitation on boundary layer dynamics is examined.

2. Experimental design

a. General model description

The model used in this study is the Large Eddy Simulation (LES) version of the Regional Atmospheric Modeling System (RAMS) model developed at Colorado State University (Pielke et al. 1992) that calculates droplet growth explicitly following the moment-conserving techniques of Tzivion et al. (1987, 1989). It is used in its two-dimensional form and as such will be termed a CRM, rather than an LES model. The model was used in an earlier study of marine stratocumulus clouds (Feingold et al. 1994a) and has since been improved by including positive-definite, monotonic advection operators for all of the scalars. Only a brief model description is provided here, with details furnished in Stevens et al. (1996).

The model is nonhydrostatic and compressible. It solves prognostic equations for two velocity components (u, w), liquid-water potential temperature, θ_l, perturbation Exner function π, and total water-mixing ratio r_t. The explicit microphysical routines require an additional 50 prognostic equations for both the number and mass concentrations in each of the 25 size bins. The processes of drop condensation–evaporation, collection (through solution to the stochastic collection equation), and sedimentation are all taken into account. In addition, we predict six size categories of CCN (as described in Cotton et al. 1993). These bins are defined in terms of supersaturation with bin bounds at 1%, 0.6%, 0.3%, 0.1%, 0.02%, and 0%. The scheme is based on Twomey's (1959) relationship

$$N_a = CS^k, \tag{1}$$

where N_a is the number of activated CCN, C and k are empirically measured parameters, and S is the supersaturation. Within each bin, an apparent supersaturation dependence of k is allowed based on measurements of Hudson and Frisbie (1991), and C varies according to the number of CCN present. On complete evaporation of a drop, one CCN particle is regenerated (Mitra et al. 1992) in a manner that globally conserves the shape of the CCN spectrum (in the absence of collection and sedimentation) (Cotton et al. 1993).

b. Specific modifications for this study

The decision to run the model as a CRM rather than an LES is due primarily to the enormous computational costs of three-dimensional simulations. However, because the set of experiments performed here only examine the sensitivity of drizzle formation to cloud vertical velocity, and the simulations are not intended to be a definitive case study, this should not detract from the results. We expect three-dimensional results to differ quantitatively but not qualitatively from those presented here.

The model is initialized with a sounding taken from the research vessel *Malcolm Baldridge* at 0705 UTC 16 June 1992. On the day in question, a solid cloud deck covered the skies and drizzle was recorded during the early morning. Using this sounding, the model reproduced the location of cloud top and cloud base in good agreement with observations and generated drizzle for a range of CCN concentrations (Feingold et al. 1994b). The grid size is 55 m in the horizontal and varies in the vertical between 25 m (near the surface and at cloud top) to 50 m (within the cloud). Above

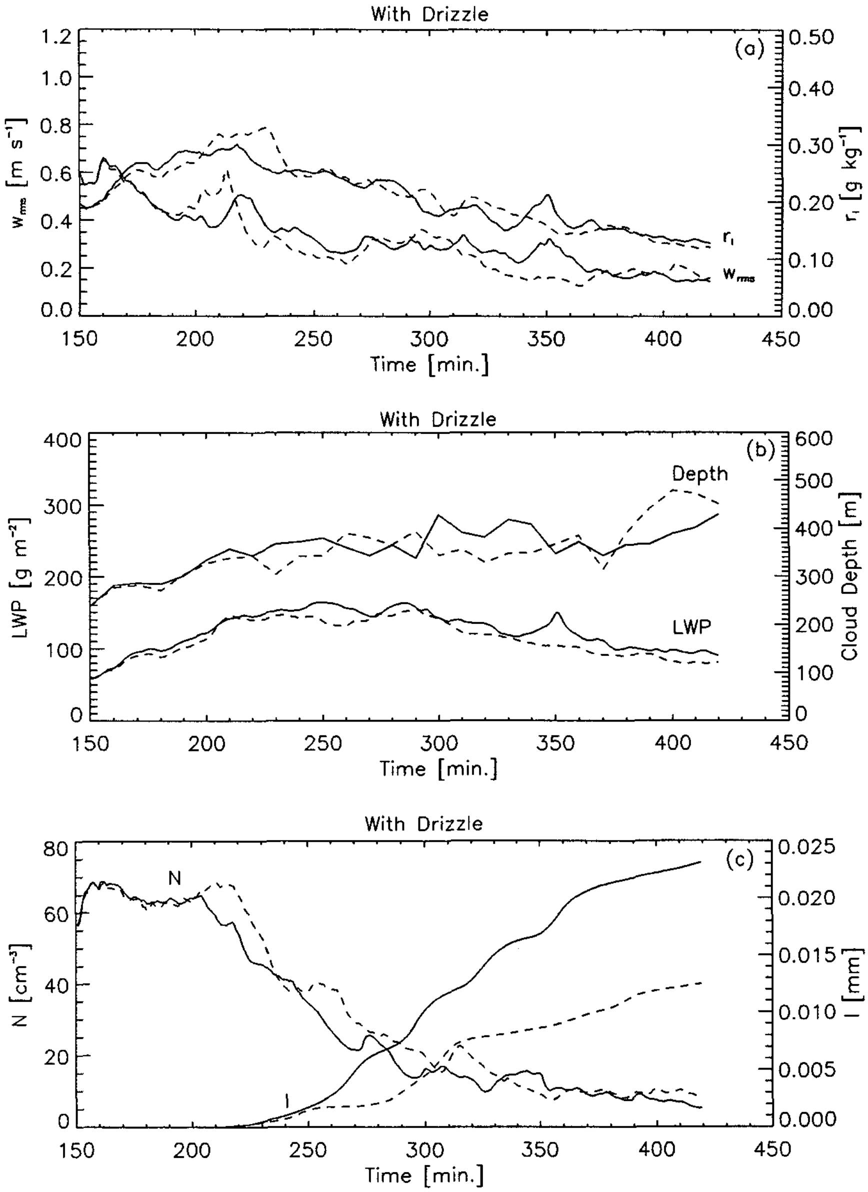

FIG. 2. Temporal evolution of (a) w_{rms} and r_l and (b) LWP and cloud depth. (c) Number concentration N and integrated rain at the surface I for the precipitating case. Line types are as in Fig. 1.

cloud top, there is a 10% grid stretching from one level to the next. Sea surface temperature is fixed at 17.6°C, that is, the same temperature as the lowest model grid point at the initial time. Boundary conditions are cyclic in the horizontal, with a rigid lid at the model top and a Rayleigh friction wave-absorbing layer. Longwave radiative forcing is parameterized using the Chen and Cotton (1983) scheme, which responds to bulk cloud water content. In order to simplify the calculations, and, again, since this work is not intended as a case study, shortwave radiation is not simulated. A 2-s time step is used for all but the acoustic terms.

3. Results

The main conclusion of Bowen's (1950) study is that the trajectory of the collector drop is dependent on (a) the updraft velocity and (b) the cloud liquid water content. An analogous study in the current environment can be designed in such a way that the model produces clouds that exhibit varying degrees of vigour and liquid water contents. This can be achieved in a number of ways—one of the most straightforward being to apply varying rates of longwave cooling at cloud top; stronger cooling should drive stronger circulations and

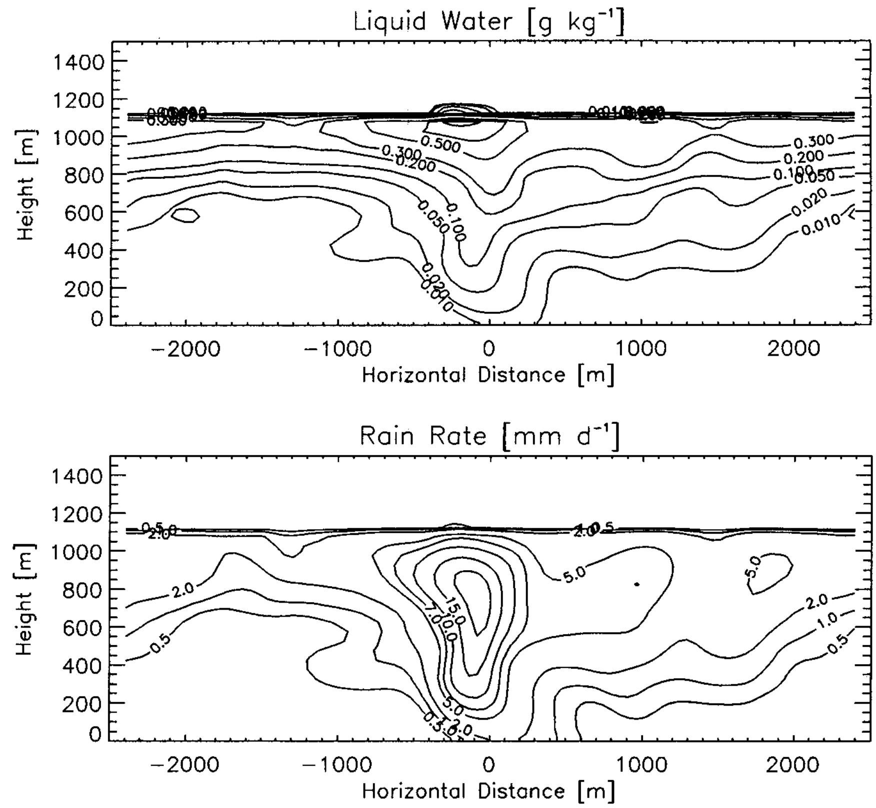

FIG. 3. Contour plots of (a) r_l (g kg^{-1}) and (b) R (mm d^{-1}) 320 minutes into the simulation of the base case. A strong drizzle event is evident in the center of the domain.

produce deeper and wetter clouds. An example of this is shown in Fig. 1 for runs where a simple bulk liquid water condensation scheme is used and no precipitation is allowed. Two runs are performed and differ only in the longwave forcing applied during the last 150 min; the first has a cooling rate at cloud top of about 6.5 K h^{-1} and is approximately 15% larger than the second. Figure 1 shows the time evolution of the root-mean-square velocity $w_{\rm rms}$, cloud water mixing ratio r_l, liquid water path (LWP), and cloud depth.[1] In both cases cloud cover is 100% throughout the period of comparison. The case with weaker longwave forcing exhibits smaller values of all fields in accordance with longwave radiation being a primary driving force. On average the decrease is 20% in $w_{\rm rms}$, 7% in r_l, 15% in LWP, and 7% in cloud depth.

These same experiments are rerun, but this time detailed microphysical calculations are performed and precipitation *is* allowed. The results (Fig. 2) show a number of interesting differences from those in Fig. 1; the $w_{\rm rms}$ fields exhibit different structures, although their time-average values differ by only 5% and the time-average r_l fields are almost identical. On average, the run with weaker forcing shows a decrease in LWP of 9%, an increase in number concentration N of about 9%, and a decrease in cloud depth of less than 1%. Despite these rather modest differences, the difference in the amount of drizzle reaching the surface is substantial; the time-integrated drizzle amount I at the surface is 85% larger for the case with stronger longwave forcing.

These results suggest that (a) drizzle formation is related to the intensity of the circulations, and (b) the drizzle process has important feedbacks to the model dynamics. Regarding the former, clouds with larger TKE are expected to be able to support droplets in cloud for longer periods of time and therefore prolong collision–coalescence, and thus generate more drizzle. Regarding the latter, Fig. 2a exhibits $w_{\rm rms}$ values that are significantly smaller than those in Fig. 1a. In addition, the difference in $w_{\rm rms}$ values between the stronger and weaker longwave runs in Fig. 2a is far smaller than that difference in Fig. 1a.

Unfortunately, the complex feedbacks in these simulations (e.g., the redistribution of heat and vapor due

[1] The threshold for cloud is defined in this study as the point at which r_t just saturates the air at θ_l. A threshold based on LWC is too sensitive to drizzle and does not give a physically meaningful representation of cloud boundaries.

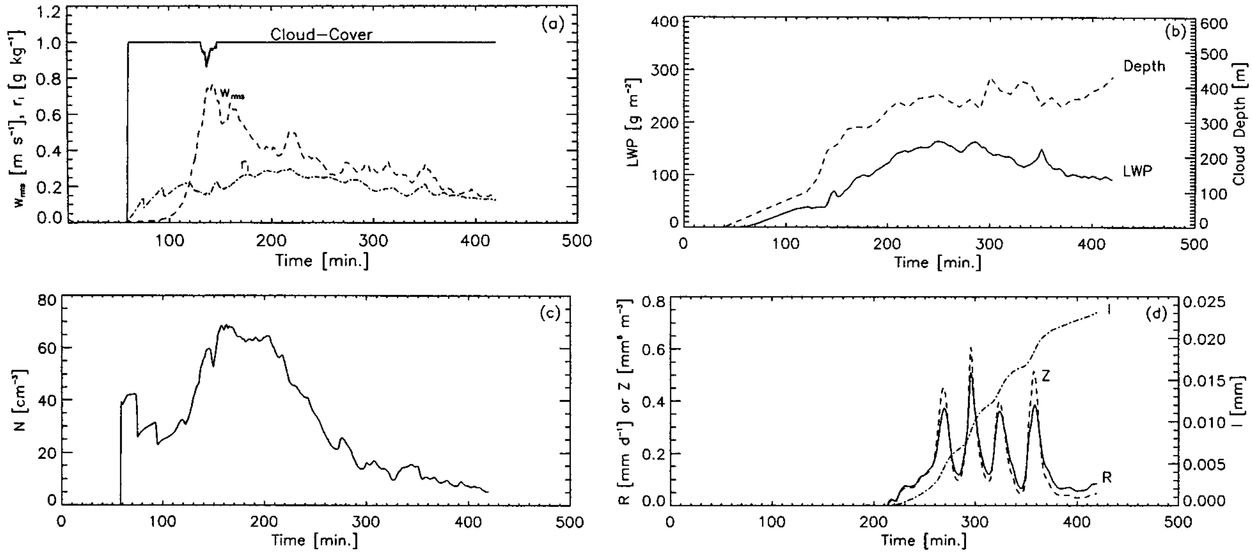

FIG. 4. Temporal evolution of (a) w_{rms}, r_l, and cloud cover; (b) cloud depth and LWP (g m^{-2}); (c) N (cm^{-3}); and (d) surface values of R (mm d^{-1}), Z (mm^6 m^{-3}), and I (mm).

to the drizzle process, modification to longwave cooling as a result of enhanced or depleted LWC) preclude direct conclusion about the extent to which drizzle formation is related to TKE and in-cloud residence times. In order to isolate the latter effect, a series of experiments is proposed in which a fixed dynamical framework is imposed on the BL and no feedback of drizzle to the dynamics is allowed. Droplets then follow similar trajectories until their terminal velocities exceed the updraft velocity. This set of experiments is then repeated, but this time the microphysics and dynamics are coupled. The design of these experiments is elaborated upon below.

a. Modification of the drop terminal velocities

The primary factor determining the residence time of a drop in cloud is the velocity of the drops *relative to the cloud velocities.* The net vertical motion of a droplet is given by the difference between the local updraft velocity w and the drop terminal velocity V_T (defined as positive downward):

$$w_{\text{net}} = w - V_T. \qquad (2)$$

Thus, the simulation of a more vigorous cloud with, say, $w \pm \epsilon$ is equivalent (in terms of w_{net}) to the simulation of that cloud with the same w but terminal velocity $V_T \mp \epsilon$:

$$(w \pm \epsilon) - V_T = w - (V_T \mp \epsilon). \qquad (3)$$

Based on this principle, an amount ϵ can simply be added to or subtracted from each drop terminal velocity to simulate smaller or larger w. This method does not compromise calculation of fall distances of drops relative to one another, or their coalescence growth—both being dependent on a conservation of the difference in the terminal velocities ΔV_T.

There is, however, a practical problem in the implementation of this approach; when subtracting ϵ from V_T we find that for $V_T \leqslant \epsilon$ the applied fall velocity is negative, and droplets "fall" upward, eventually reaching the dry above-cloud air where they rapidly evaporate. To alleviate this, it will be assumed that all drops with V_T smaller than ϵ move with the cloud motions. (For symmetry, we apply this rule to all cases $V_T - \epsilon$, $V_T + \epsilon$, and V_T, although in the case of the latter two, the condition is not necessary). In the simulations where we do apply the correction to droplet fall velocity, we affect the results in the following ways: (a) the results are overly sensitive to the ability of the cloud to grow droplets above a threshold size, since at this size there is a jump in fall velocity from zero to ϵ, and (b) ΔV_T is only correct when the natural terminal velocities of the droplets exceed ϵ. (In the coalescence growth equations we still apply the correct value of ΔV_T.)

The motivation for applying corrections to fall velocities has another source: it provides some insight into the extent to which bulk microphysical parameterizations might misrepresent the drizzle process with an erroneous choice of average drop terminal velocity. There are three aspects to this problem: the first is that most drizzle parameterizations artificially differentiate between cloud droplets that move with the air motions and drizzle drops that have terminal velocity; the second relates to the assumption that one can apply a single, average fall velocity to all rain drops, whereas, in truth, no one value of terminal velocity is applicable to all drops; the third is that even if one does apply this

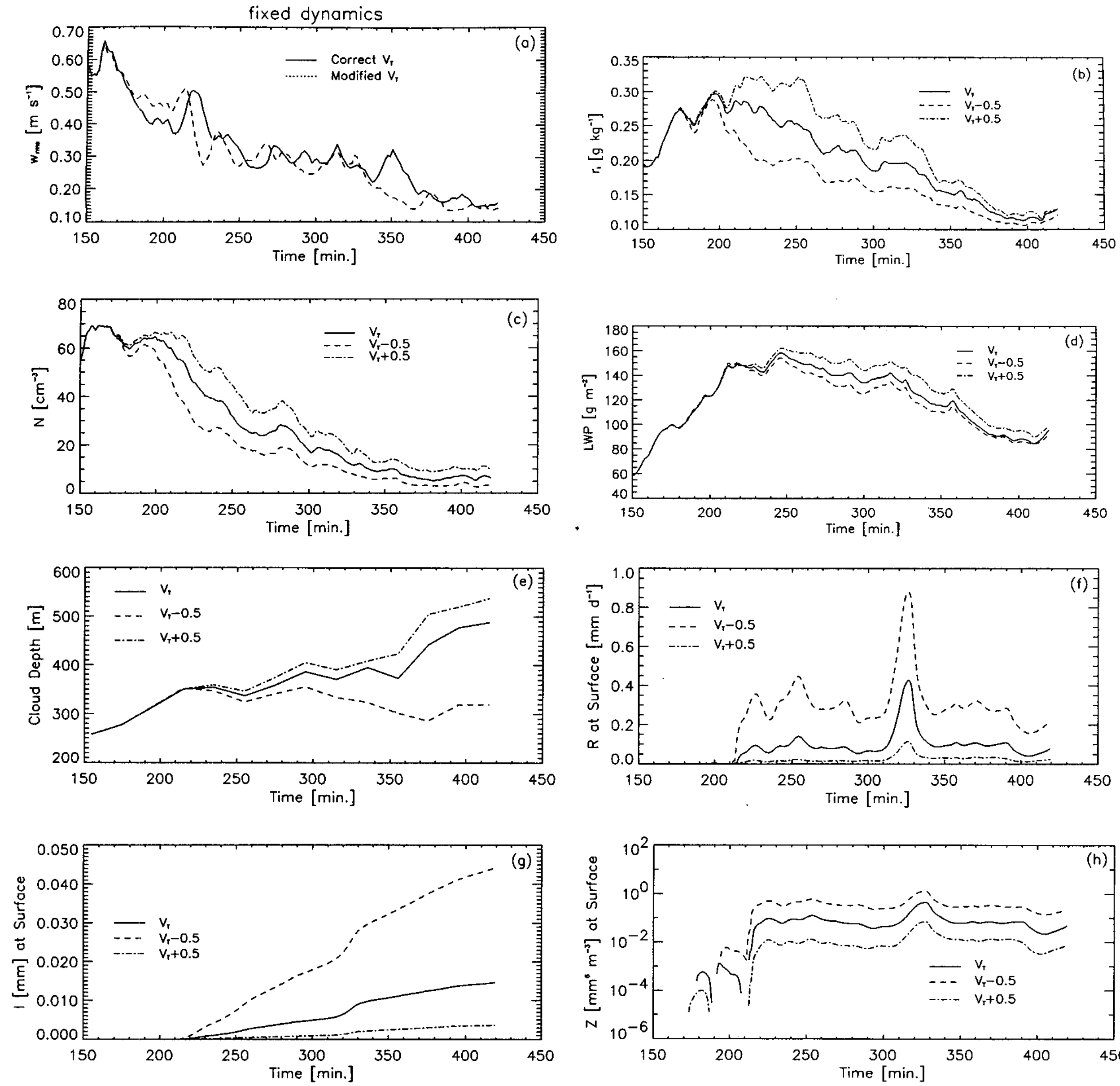

FIG. 5. Temporal evolution of various parameters for the "Bowen Model" runs. In all cases, dynamics are fixed (to that produced by run S1) and no microphysical feedback is allowed: (a) w_{rms} (for the base case and S1 runs); (b) r_l; (c) N; (d) LWP; (e) cloud depth; (f) R at the surface; (g) integrated rain at the surface, I; and (h) radar reflectivity, Z, calculated from drop spectra at the surface.

single fall velocity to all drops, one must in some cases (e.g., Kessler 1969; Chen and Cotton 1987) make some arbitrary choice for this fall velocity. (Bulk schemes that predict both mass and number of droplets do not face this second dilemma.) In this study, a size-dependent fall velocity is applied to each drop bin. The simulations that require V_T to be zero below the threshold ϵ will serve to elucidate the extent to which neglect of cloud droplet terminal velocities is of consequence. The sensitivity of the results to the artificial modification in fall velocity will indicate the importance of correct representation of fall velocity in the growth of drizzle drops.

Thus, although the proposed method of studying drizzle has its limitations, its strength lies in enabling us to examine the question of how dwell time in the cloud affects drizzle production.

b. Base case

The base case is the run with full microphysics and with the stronger longwave forcing shown in Fig. 2. It

TABLE 1. Summary of numerical experiments.

Experiment	V_T ($r < 60$ μm)	V_T ($r > 60$ μm)	Coupled microphysics–dynamics
Base case	V_T	V_T	Yes
S1	0	V_T	Yes
S2	0	$V_T - 0.5$	No (dynamics from S1)
S3	0	$V_T + 0.5$	No (dynamics from S1)
S4	0	$V_T - 0.5$	Yes
S5	0	$V_T + 0.5$	Yes

simulates cloud formation using the correct terminal velocities *for all drops* and sets the stage for the subsequent sensitivity studies. The initial CCN concentrations are 134 cm^{-3} (at 2% supersaturation) throughout the domain. In Fig. 3a, a view of the liquid water field r_l is shown after 320 minutes of simulation time during the course of a strong drizzle event. (The r_l field represents the cloud water plus drizzle water mixing ratios, unlike bulk parameterizations which differentiate between the two.) The maximum values occur at cloud top and are of the order of 0.7 g kg^{-1}. Rain rate maxima peak at about 20 mm d^{-1} (Fig. 3b). The temporal evolution of various fields can be seen in Fig. 4. (Some of these results were shown in Fig. 2 but are repeated here for clarity.) The root-mean-square velocity $w_{\rm rms}$ shows a buildup of turbulence from an initially quiescent BL; $w_{\rm rms}$ achieves a maximum at about 140 minutes and thereafter decreases slowly over the course of the 7-h run. The absence of a quasi-steady $w_{\rm rms}$ is of note and in contrast to simulations of nonprecipitating clouds using the same model (e.g., Fig. 1). It is noted (Figs. 4c,d) that the onset of drizzle at the surface is preceded by a marked decrease in N. In addition, N does not achieve a steady state due to the absence of a source of CCN to balance their depletion through collection and sedimentation. Rain rate at the surface is of the order of a few tenths of a millimeter per day and has a clear periodicity of about 30 minutes. Integrated rain at the surface and radar reflectivity Z (mm^6 m^{-3}) calculated from spectra at the surface are also shown (Fig. 4d) for future comparison with sensitivity runs. Radar reflectivity is very sensitive to drop size and is thus a good indicator of the presence of large drops.

c. The Bowen model: No dynamical feedback

We now rerun the base case with a number of variations; in accordance with the discussion in section 2a, we assume that droplets with terminal velocities less than $\epsilon = 0.5$ m s^{-1} have zero terminal velocity. The value of $\epsilon = 0.5$ m s^{-1} corresponds to a drop size of approximately 60 μm in radius. It is a somewhat arbitrary choice but not restrictive in the sense that results vary only quantitatively for different choices of ϵ (see section 3d). With this assumption we run three cases summed up in Table 1: the first (S1) uses the correct V_T for all larger droplets; for the second case (S2) we subtract an ϵ of 0.5 m s^{-1} from the values of V_T (represented by $V_T - \epsilon$); for the third case (S3) we add 0.5 m s^{-1} to their values ($V_T + \epsilon$). The first case provides an interesting comparison with the base case and shows the impact of assuming that cloud droplets move with the air motions—an assumption usually applied in bulk microphysical parameterizations. The second and third cases complete the set of simulations by representing a more (or less) vigorous cloud with an enhanced (or diminished) ability to maintain droplets in the cloud.

To isolate the effect of the drop terminal velocity relative to cloud updraft velocity, we impose on S2 and S3 the identical cloud vertical velocities as produced in S1. Figures 5a–f show comparisons of results of the temporal evolution of various parameters for the V_T, $V_T - \epsilon$, and $V_T + \epsilon$ cases. Figure 5a differs from the others in that it compares the time evolution of the $w_{\rm rms}$ BL velocity for the modified V_T case (i.e., small drops move with the cloud motions but large drops fall at their correct velocities) with that of the base case (correct V_T for *all* drops). We see that the modification tends to decrease $w_{\rm rms}$, but values are usually within a few centimeters per second of one another. The $V_T - \epsilon$ case shows clouds depleted in r_l, shallower in depth and with lower LWPs than for the V_T run. On the other hand, the $V_T + \epsilon$ case exhibits enhanced r_l with higher LWPs and deeper clouds. Drop number concentrations are lower for the $V_T - \epsilon$ run and larger for the $V_T + \epsilon$ run (Fig. 5c). The differences in drizzle production between these cases are summarized by Figs. 5f,g. Drizzle rate, R, and integrated drizzle amount at the surface, I, for the $V_T - \epsilon$ run is more than double that for the V_T run, while for the $V_T + \epsilon$ run, it is less than one-half of that in the V_T run. Moreover, we see (Fig. 5h) from the traces of radar reflectivity Z that the precipitation reaching the surface in the $V_T - \epsilon$ run is in the form of larger drops (much higher Z values), while in the case of the $V_T + \epsilon$ run it is in the form of small drops (lower Z values). (Detailed plots of droplet spectra—not shown—bear this out.) There is a noticeable difference between the periodicity of rain rate in Fig. 2d and Fig. 5f (the V_T run), indicating that the assumption of allowing small drops to move with the cloud im-

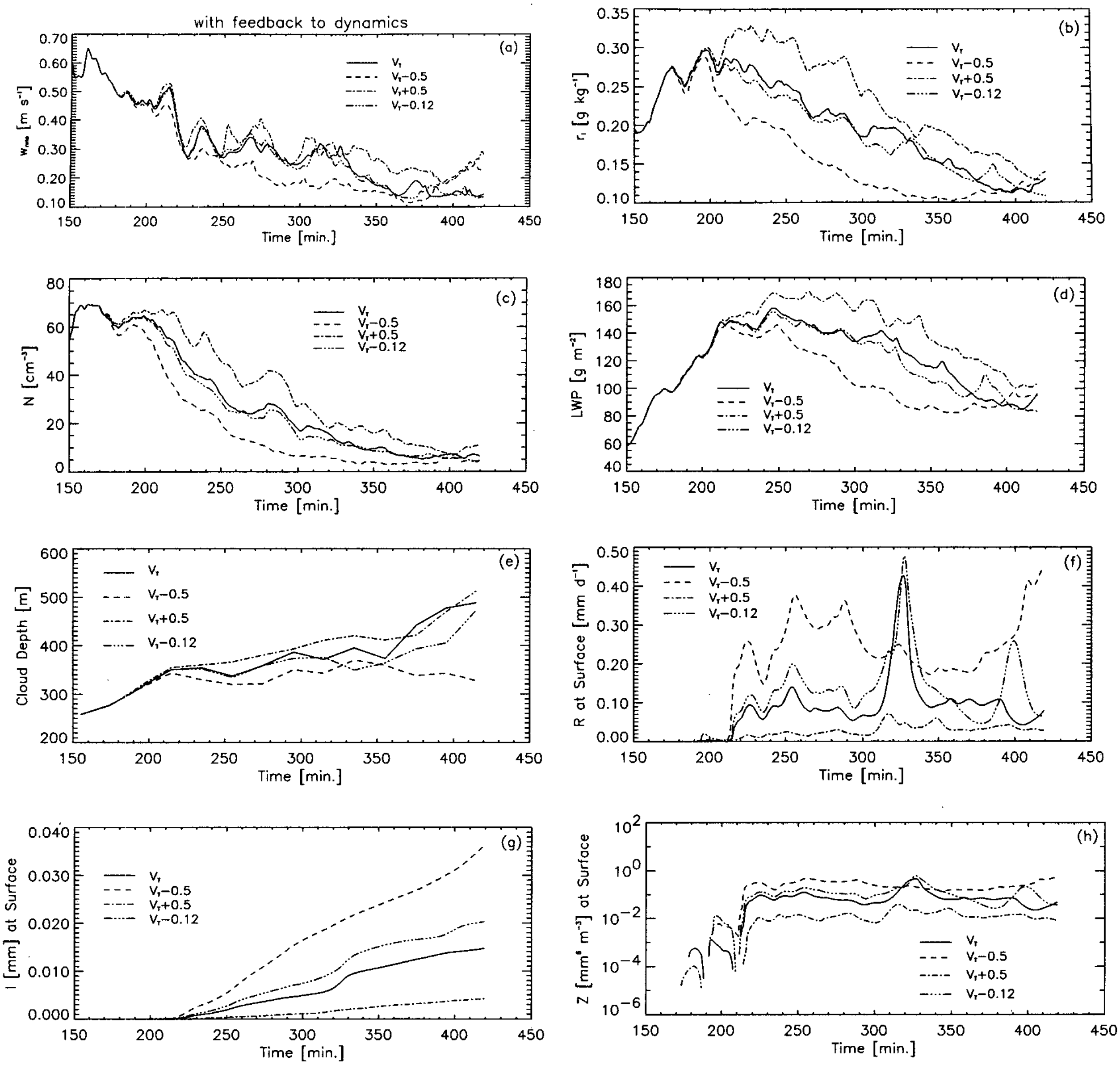

FIG. 6. Same as in Fig. 3 but with full feedback to dynamics.

pacts both the qualitative and quantitative nature of drizzle production. The extent to which this is true obviously depends on the magnitude of ϵ.

A clear picture emerges from these results. When drops have reduced fall velocities (i.e., have grown in more vigorous clouds), increased dwell time in the cloud produces more drizzle made up of larger drops. Cloud water is depleted by the drizzle process, as is cloud drop concentration and cloud depth. The converse is true for the case where drops have enhanced fall velocities (i.e., have grown in less vigorous clouds).

d. Dynamical feedback

The purpose of these experiments is to analyze the manner in which drizzle and associated processes feed back to the BL dynamics. We repeat the experiments S2 ($V_T - \epsilon$) and S3 ($V_T + \epsilon$) in section 3c, but this time we allow feedback to the dynamics (i.e., w is prognosed correctly). The $V_T - \epsilon$ and $V_T + \epsilon$ experiments with coupled dynamics will be labeled S4 and S5, respectively (Table 1). A comparison of the temporal evolution of the various fields is shown in Fig. 6. Values of $w_{\rm rms}$ (Fig. 6a) are lower for the $V_T - \epsilon$ case but higher

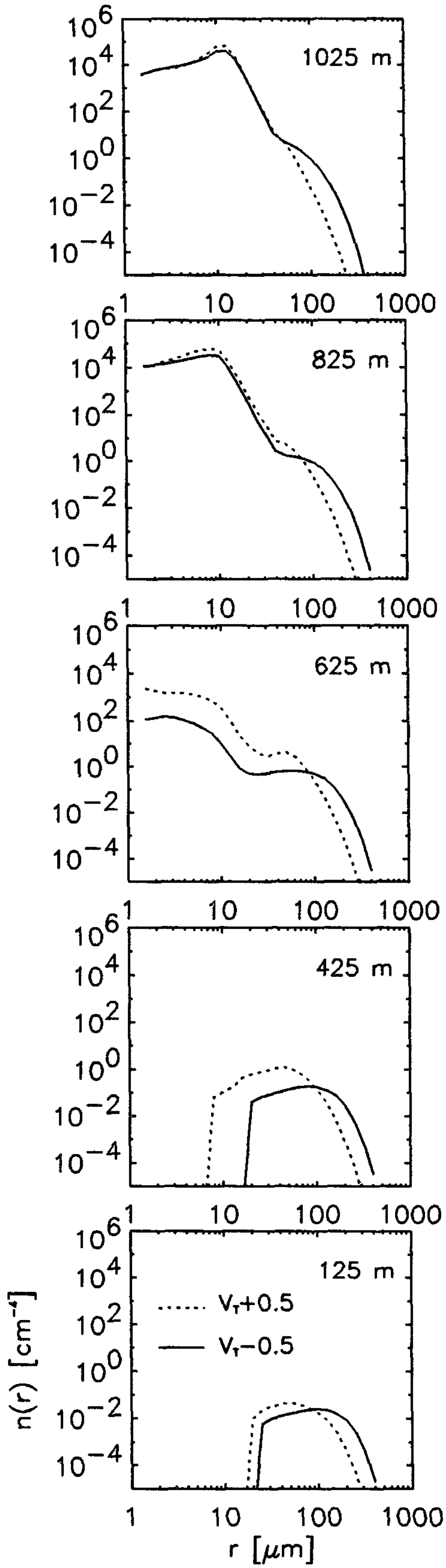

for the $V_T + \epsilon$ case. This represents a negative feedback since the $V_T - \epsilon$ run represents a more vigorous BL and the $V_T + \epsilon$ run represents a less vigorous BL (see section 5a). When compared with S1, cloud water is lower for the $V_T - \epsilon$ run and higher for the $V_T + \epsilon$ run, with concomitant changes in LWP. Here the feedback enhances the difference in LWP when compared to the runs with fixed dynamics (cf. Figs. 5d and 6d). Again, cloud depth is diminished for the $V_T - \epsilon$ and enhanced for the $V_T + \epsilon$ run. Figures 6f–h show the same trends for R, I, and Z observed in Figs. 5f,g,h, namely, that the $V_T - \epsilon$ run produces more drizzle in the form of larger drops, while the $V_T + \epsilon$ run produces less drizzle in the form of smaller drops. This is borne out by plots of horizontally averaged drop spectra taken from a snapshot of the domain at 350 minutes (Fig. 7); the spectra all show evidence of a drizzle-drop mode at around 100 μm. Through the depth of the cloudy air and subcloud drizzle, the $V_T - \epsilon$ spectra point to the existence a stronger collection process, with higher concentrations of drops > 100 μm than their $V_T + \epsilon$ counterparts.

Qualitatively these same cloud microphysical features were evident in the runs with fixed dynamics, and only their magnitude is affected by the coupling with the dynamics. Thus, the dominant effect is the fall velocity of the drops relative to cloud vertical velocity, and feedbacks are not sufficient to erase this effect.

Also shown in Fig. 6 are the results for an adjustment in V_T in the amount $\epsilon = 0.12$ m s^{-1}, which corresponds to a droplet radius of about 32 μm. The $w_{\rm rms}$, r_l, LWP, and cloud depth fields are close in magnitude to those for the V_T case, with a tendency to be a few percent lower. The notable exception is the drizzle related fields where there is a 38% enhancement in I at the end of the simulation. This run provides confidence in the robustness of the results.

4. Discussion

The results have demonstrated that the production of drizzle in stratocumulus clouds is closely related to the ability of the cloud to maintain droplets within its bounds and allow greater time for collision–coalescence.[2] It is not suggested that the number con-

[2] The time available for condensational growth will also be enhanced, but this factor by itself is expected to be of secondary importance.

FIG. 7. Horizontally averaged drop spectra as a function of height at 250 minutes. The solid lines pertain to the $V_T - \epsilon$ run, while the dashed lines pertain to the $V_T + \epsilon$ run (runs S4 and S5, respectively, including dynamical feedback). Spectra from the $V_T - \epsilon$ run exhibit more drops greater than 100 μm than those in the $V_T + \epsilon$ run.

centration of CCN is an insignificant parameter in drizzle production but rather that dynamical factors also play a significant role. The collision–coalescence process is determined by the droplet spectrum (characterized for example by LWC and N), as well as time; for a given cloud LWC, the CCN concentration will largely determine the number of activated droplets, whereas the dynamics will determine the dwell time in the cloud. Thus, both microphysical and dynamical factors are important. The parameterization of drizzle in mixed-layer models is typically in terms of droplet number and cloud depth (e.g., Pincus and Baker 1993). These results suggest that if models of this type are to predict drizzle production successfully, some measure of the cloud TKE may be required in conjunction with cloud depth to give a characteristic time τ available for collision–coalescence. For example, this might have the form

$$\tau = A \frac{\text{cloud depth}}{(\text{TKE})^{1/2}}, \tag{4}$$

where A is an undetermined constant. The validity of (4) has not been tested.

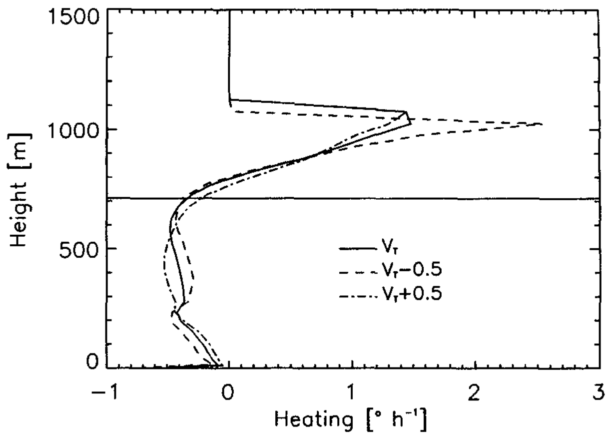

FIG. 8. Horizontally averaged profiles of heating associated with the drizzle flux (calculated from the vertical divergence of the drizzle flux) for the V_T, $V_T - \epsilon$, and $V_T + \epsilon$ cases. The $V_T - \epsilon$ run shows stabilization relative to the V_T run, while the $V_T + \epsilon$ run shows relative destabilization. The solid horizontal line represents an average level of cloud base.

a. Impact of drizzle on boundary-layer dynamics

The experiments that investigate the manner in which drizzle feeds back on to BL dynamics (section 3d) beg further analysis. In Fig. 8, we show horizontally averaged profiles of the heating associated with the drizzle (calculated from the divergence of the drizzle flux). Profiles are averaged over 210 minutes to obtain better statistics. Also plotted is the average cloud-base height for the V_T run. It can be seen that there is a small region above the average level of cloud base where evaporative cooling does exist; this is a consequence of the temporal averaging of a gradually lowering cloud base. The profiles show that in the case of the $V_T + \epsilon$ run, the strongest cooling associated with evaporation is in the region just below cloud base, while the $V_T - \epsilon$ run shows the strongest cooling at the surface. Relative to the V_T run, the $V_T + \epsilon$ run produces stronger destabilization of the BL and tends to produce deeper circulations (Fig. 9b). In contrast, the $V_T - \epsilon$ run produces a stronger stabilization of the BL; cooling in the region just below base is weaker than in the V_T run, while cooling near the surface is stronger. The resulting circulations are weaker and tend to be confined to two levels (Fig. 9a). If one averages the w_{rms} values for this same 210-min period and plots the values as a function of the average cooling below cloud base associated with drizzle (i.e., the average value associated with the profiles in Fig. 8), we see (Fig. 10) that there is no clear dependence of w_{rms} on subcloud cooling. Rather, it is the *distribution* of this cooling with height that is critical to generating the stronger, deeper circulations. This result stresses the importance of accurate calculations of the distribution of evaporative cooling. Models that employ explicit microphysical schemes are better suited to do this and in this regard should have an advantage over models that use bulk-microphysical parameterizations.

The contrast between the runs in Fig. 1 (no drizzle) and Fig. 2 (with drizzle) for two different longwave forcings also elucidates the impact of drizzle on the BL. In the absence of drizzle, the cloud tends to be wetter and more energetic when longwave forcing is stronger. However, although these trends are also evident when drizzle is present (Fig. 2), the sensitivity to longwave forcing is reduced. (This is most noticeable in the r_l field.) Thus, the inclusion of drizzle tends to feed back in a manner that diminishes the boundary layer TKE and cloud r_l when drizzle is enhanced. Figure 6 offers similar evidence of this; the $V_T - \epsilon$ run exhibits much lower w_{rms} and r_l than the V_T run. (Despite these weak velocities, the cloud still manages to produce large amounts of drizzle because the fall velocities are strongly diminished.) Conversely, the results for $V_T + \epsilon$ show (Fig. 6) enhanced values of w_{rms} and r_l in conjunction with smaller amounts of drizzle.

b. Dynamical feedback, fixed radiative forcing

For the runs in section 3d (Fig. 6), all fields were coupled in the correct manner. This raises the question as to the influence of longwave radiative cooling in the feedback to the dynamics. For example, it is not clear whether the enhanced BL velocities for the $V_T + \epsilon$ run in Fig. 6a are produced by the larger values of r_l and subsequent enhanced longwave cooling or by evaporative cooling of drizzle below cloud base. For this reason, the experiments in section 3c (Fig. 6) were re-

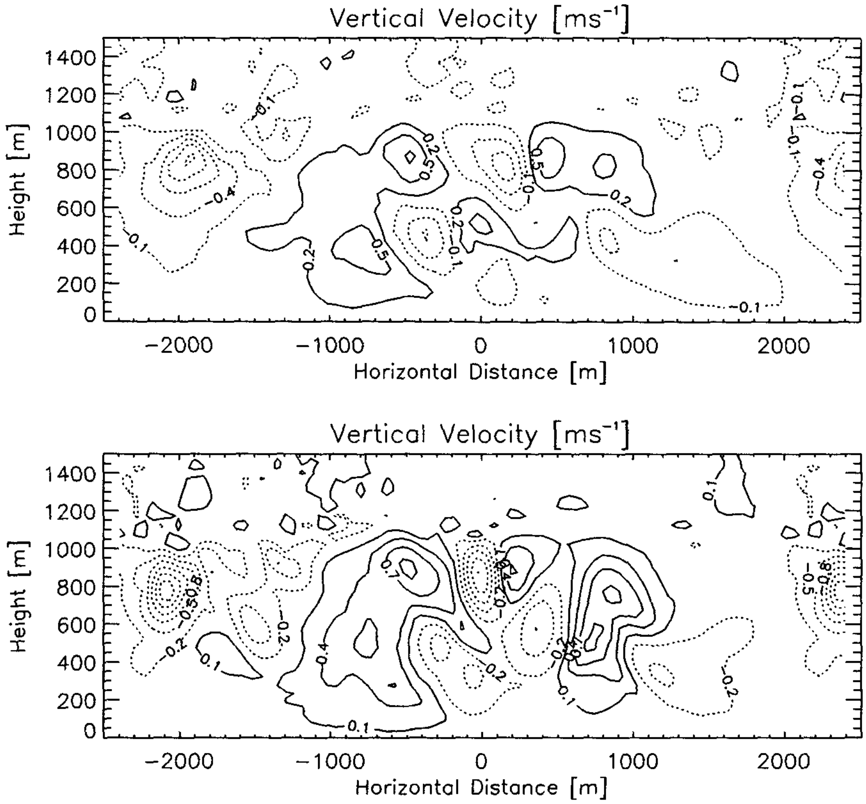

FIG. 9. Contour plots of vertical velocity at 230 minutes (a) for the $V_T - \epsilon$ run and (b) for the $V_T + \epsilon$ run. Dashed lines indicate downdrafts and solid lines updrafts. Contour interval is 0.3. Here (a) exhibits weaker circulations (maximum 0.8 m s^{-1} and minimum -1.3 m s^{-1}), while (b) shows stronger, deeper circulations (maximum 1.1 m s^{-1} and minimum -1.9 m s^{-1}).

peated, but this time with the magnitude of longwave radiation fixed for the entire duration of the three runs (V_T, $V_T - \epsilon$, and $V_T + \epsilon$). (The values used correspond to those generated for the V_T run at $t = 150$ minutes.) With the equivalent longwave forcing, the differences between the three runs are qualitatively the same (and quantitatively similar) as the results presented in Fig. 6 and are therefore not shown. We can therefore conclude that the observed response is not established by radiative feedbacks.

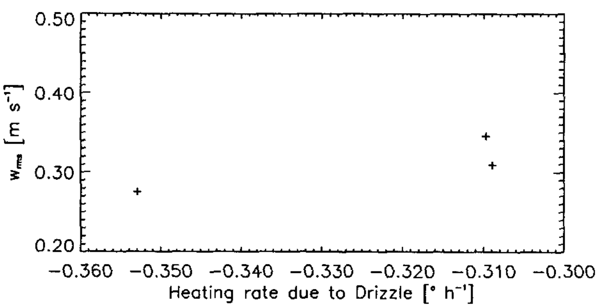

FIG. 10. Time-averaged w_{rms} as a function of time-averaged heating associated with the drizzle flux for the V_T, $V_T - \epsilon$, and $V_T + \epsilon$ runs in Fig. 4.

c. Comparison to the effect of reducing CCN concentrations

It is well known that drizzle production is a function of the CCN concentration and size spectrum (although this effect has yet to be well quantified by measurements and modeling studies). In order to place the relative importance of these two effects into perspective, we run the base case with less than one-half the original CCN concentration; the shape of the activation spectrum is the same as in the base case, but the concentration activated at 2% supersaturation is reduced from 134 to 55 cm^{-3}. We show only the time series of R, I, and Z at the surface for comparison with Fig. 4. It is evident (Fig. 11) that the enhancement of rain rate at the surface is sometimes significant, with peak rain rates exceeding 2.5 mm d^{-1}. These peak values of R (and Z) are higher than any achieved by varying the drop terminal velocities. On the other hand, a comparison of the integrated rain at the surface shows that the enhancement as-

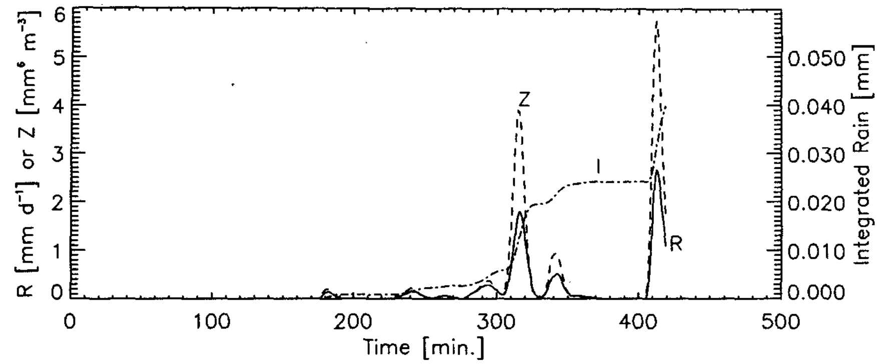

FIG. 11. Time series of surface R, I, and Z for the sensitivity run using lower values of CCN (55 cm^{-3}).

sociated with halving the CCN concentration is comparable to the impact of the $V_T - \epsilon$ experiment (cf. Fig. 11 and Fig. 6g). Thus, although more rigorous study must be carried out in order to quantify these effects, it is clear that the effect of TKE, as a means of prolonging collision–coalescence, cannot be neglected as a factor in drizzle formation.

d. Relationship between drizzle production and cloud depth

Cloud depth has a strong impact on radiative transfer and as such deserves some attention in the framework of this study. Moreover, the work of Pincus and Baker (1994) shows that there is potentially an important link between cloud drop number, drizzle production, and cloud depth. Based on steady-state results from a mixed-layer model, Pincus and Baker (1994) hypothesized that cloud depth increases with increasing droplet concentration (and decreasing drizzle production). In their calculations, the increase in cloud depth is primarily due to an elevated cloud top, with relatively small variations in cloud base.

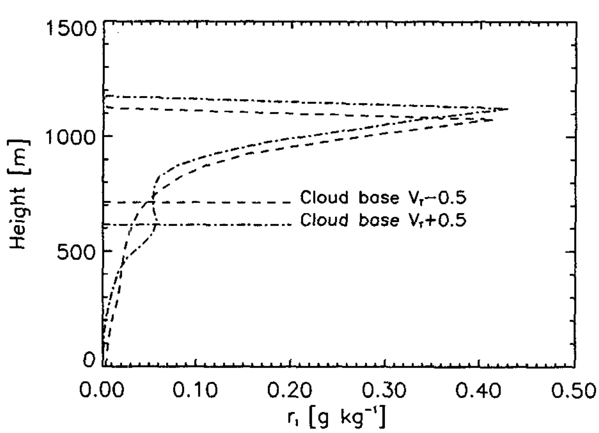

FIG. 12. Horizontally averaged profiles of r_l at t = 420 minutes for the runs in Fig. 6. The short, horizontal lines indicate the level of cloud base calculated using the thermodynamic criterion.

In the current work, cloud depth has been calculated using a thermodynamic criterion based on the point at which the total mixing ratio r_t just saturates the air at θ_l. Although qualitatively similar values of cloud depth are arrived at using a definition based on a threshold of N = 0.1 cm^{-3}, a definition based on a liquid water mixing ratio threshold of 0.02 g kg^{-1} strongly biases the results such that clouds producing more drizzle are invariably deeper than those producing less drizzle. Examination of Figs. 5e and 6e shows that the difference in cloud depth between the $V_T + \epsilon$ and $V_T - \epsilon$ runs increases steadily, and by the end of the runs is on the order of 200 m. Analysis of the data shows that this difference is associated mainly with the level of cloud base. Figure 12 shows horizontally averaged profiles of the r_l field at the end of the runs in Fig. 6, as well as the location of the respective cloud bases calculated using the thermodynamic criterion. The use of an r_l threshold would clearly place cloud base quite differently. Figure 12 highlights the fact that conclusions regarding the correlation between various parameters and cloud depth for these poorly mixed boundary layers are likely to be highly sensitive to the manner in which cloud base is defined. In contrast, mixed-layer models have well defined cloud bases (Pincus and Baker 1994), but it is not clear how well the assumption of a well mixed layer applies for drizzling clouds.

e. A possible time evolution of drizzle formation

The numerical experiments S1, S4, and S5 (coupled microphysics and dynamics) present evidence of a possible cause and effect mechanism in drizzle production.

The following hypothesis is offered: as droplets grow in the cloud and reach a point at which they cannot be sustained by the cloud velocities, they begin to fall below cloud base where they evaporate. During the initial phases of drizzle fallout, we expect these drops to contribute little to total cloud water and to be small in number. They will likely evaporate in the region close to cloud base in a manner similar to case S5 ($V_T + \epsilon$). The result will be a relative destabilization of the subcloud layer and subsequent strengthening of boundary-layer velocities. This could result in enhanced cloud liquid water (with stronger circulations aided perhaps by increased longwave cooling), a stimulated collision–coalescence growth mechanism, and a positive feedback to drizzle formation. With increasing amounts of drizzle in the form of larger drops being produced, more drops are expected to survive the fall in the subsaturated air below cloud base. By analogy to case S4 ($V_T - \epsilon$), evaporative cooling will then dominate at the surface (e.g., Paluch and Lenschow 1991), resulting in a relative stabilization of the BL and a negative feedback to further drizzle production. We plan to perform further numerical experiments, as well as examine measurements using NOAA K_α-band radar from the ASTEX experiment (Frisch et al. 1995), to test this hypothesis.

5. Summary and conclusions

The experiments shown here only touch on the myriad of issues associated with the study of drizzle. They have highlighted the extent to which the droplet terminal velocity *relative* to the updraft velocity is critical in determining drizzle production and underscore the importance of incorporating a characteristic time available for collision–coalescence in drizzle parameterizations. It is noted that these results could only be produced using microphysics that explicitly resolve drop sizes and with a model that reasonably resolves the spatial distribution of boundary-layer vertical velocities. Although these results were obtained in a two-dimensional framework, they are expected to be qualitatively valid for natural (three-dimensional) clouds.

In analogy to the Bowen model, this study concludes the following.

- Clouds that are more vigorous can support droplets longer and allow for repeated collision–coalescence cycles. The drizzle drops that fall below the cloud are larger and have a greater chance of reaching the surface.

The results associated with the impact of drizzle on BL dynamics suggest the following.

- When drizzle is substantial and in the form of large drops, cooling is spread over the depth of the subcloud layer. Substantial evaporative cooling near the surface tends to stabilize the boundary layer.
- When drizzle is in the form of small drops, subcloud evaporation is more efficient and cooling will tend to be confined to the uppermost part of the subcloud region, resulting in destabilization of the boundary layer.

We have shown that in contrast to results from mixed-layer models (Pincus and Baker 1994) cloud depth is mainly controlled by the height of cloud base. The choice of method used to calculate cloud base has a significant impact on cloud depth, making it difficult to draw conclusions about the relationship between cloud depth, drop number, and drizzle. This subject will be the focus of future work.

Finally, the results show that the impact on drizzle production of a cloud's ability to enhance collision–coalescence by increasing in-cloud dwell-time is of similar order to that of substantially reducing CCN concentrations. Quantifying these relative effects will require further numerical experiments and observations.

Acknowledgments. This research was partially funded by the U.S. Department of Energy's (DOE) National Institute for Global and Environmental Change (NIGEC) through the NIGEC South Central Regional Center at the Tulane University under contract TUL-021-94/95. (DOE Cooperative Agreement number DE-FC03-90ER61010.) Additional support came from a DOE grant under the proposal entitled "Shipboard measurements of the cloud capped marine boundary layer during FIRE/ASTEX." Financial support does not constitute an endorsement by DOE of the views expressed in this article/report. Bjorn Stevens is a recipient of the NASA/EOS Global Change Fellowship under Contract NGT-30231.

REFERENCES

Albrecht, B. A., 1989: Aerosols, cloud microphysics, and fractional cloudiness. *Science,* **245,** 1227–1230.

——, 1993: Effects of precipitation on the thermodynamic structure of the trade wind boundary layer. *J. Geophys. Res.,* **98,** 7327–7337.

Austin, P. H., Y. Wang, R. Pincus, and V. Kujala, 1995: Precipitation in stratocumulus clouds: Observational and modelling results. *J. Atmos. Sci.,* **52,** 2329–2352.

Bowen, E. G., 1950: The formation of rain by coalescence. *Aust. J. Sci. Res. A,* **3,** 193–213.

Brost, R. A., J. C. Wyngaard, and D. H. Lenschow, 1982: Marine stratocumulus layers. Part II: Turbulence budgets. *J. Atmos. Sci.,* **39,** 818–836.

Chen, C., and W. R. Cotton, 1983: A one-dimensional simulation of the stratocumulus-capped mixed layer. *Bound.-Layer Meteor.,* **25,** 289–321.

——, and ——, 1987: The physics of the marine stratocumulus-capped mixed layer. *J. Atmos. Sci.,* **44,** 2951–2977.

Cotton, W. R., B. Stevens, G. Feingold, and R. L. Walko, 1993: Large eddy simulation of marine stratocumulus cloud with explicit microphysics. *ECMWF/GCSS Workshop on Parameterization of the Cloud Topped Boundary Layer,* Reading, United Kingdom, ECMWF.

Cox, S. K., D. S. McDougal, D. Randall, and R. Schiffer, 1987: FIRE—The First ISCCP Regional Experiment. *Bull. Amer. Meteor. Soc.,* **68,** 114–118.

de Almeida, F. C., 1976: The collisional problem of cloud droplets moving in a turbulent environment. Part I: A method of solution. *J. Atmos. Sci.,* **33,** 1571–1578.

Deardorff, J. W., 1980: Cloud-top entrainment instability. *J. Atmos. Sci.,* **37,** 131–147.

Feingold, G., B. Stevens, W. R. Cotton, and R. L. Walko, 1994a: An explicit cloud microphysical/LES model designed to simulate the Twomey effect. *Atmos. Res.,* **33,** 207–233.

——, A. S. Frisch, B. Stevens, and W. R. Cotton, 1994b: Simulations of marine stratocumulus clouds during ASTEX: Comparisons with radar/radiometer measurements. *Second Int. Conf. on Air–Sea Interaction and Meteorology and Oceanography of the Coastal Zone,* Lisbon, Portugal, Amer. Meteor. Soc., 44–45.

Frisch, A. S., C. W. Fairall, and J. B. Snider, 1995: On the measurement of stratus cloud and drizzle parameters with a K_α-band Doppler radar and a microwave radiometer. *J. Atmos. Sci.,* **52,** 2788–2799.

Hudson, J. G., and P. R. Frisbie, 1991: Cloud condensation nuclei near marine stratus. *J. Geophys. Res.,* **96,** 20 795–20 808.

Johnson, D. B., 1980: The role of giant and ultragiant aerosol particles in warm rain initiation. *J. Atmos. Sci.,* **39,** 448–460.

Kessler, E., 1969: *On the Distribution and Continuity of Water Substance in Atmospheric Circulation, Meteor. Monogr.* No. 32, Amer. Meteor. Soc., 84 pp.

Kogan, Y. L., D. K. Lilly, Z. N. Kogan, and V. V. Filyushkin, 1994: The effect of CCN regeneration on the evolution of stratocumulus layers. *Atmos. Res.,* **33,** 137–150.

——, M. P. Khairoutdinov, D. K. Lilly, Z. N. Kogan, and Q. Liu, 1995: Modelling of stratocumulus cloud layers in a large eddy simulation model with explicit microphysics. *J. Atmos. Sci.,* **52,** 2923–2940.

Lilly, D. K., 1968: Models of cloud-topped mixed layers under a strong inversion. *Quart. J. Roy. Meteor. Soc.,* **94,** 292–309.

Martin, G. M., D. W. Johnson, D. P. Rogers, P. R. Jonas, P. Minnis, and D. A. Hegg, 1995: Observations of the interaction between cumulus clouds and warm stratocumulus clouds in the marine boundary layer during ASTEX. *J. Atmos. Sci.,* **52,** 2902–2922.

Mason, B. J., 1952: Production of rain and drizzle by coalescence in stratiform clouds. *Quart. J. Roy. Meteor. Soc.,* **78,** 377–386.

Mitra, S. K., H. R. Pruppacher, and J. Brinkmann, 1992: A windtunnel study on the drop-to particle conversion. *J. Aerosol Sci.,* **23,** 245–256.

Moeng, C.-H., 1986: Large-eddy simulation of a stratus-topped boundary layer. Part I: Structure and budgets. *J. Atmos. Sci.,* **43,** 2886–2900.

Nicholls, S., 1984: The dynamics of stratocumulus. *Quart. J. Roy. Meteor. Soc.,* **110,** 821–845.

——, 1987: A model of drizzle growth. *Quart. J. Roy. Meteor. Soc.,* **113,** 1141–1170.

Oliver, D. A., W. S. Lewellen, and G. G. Williamson, 1978: The interaction between turbulent and radiative transport in the development of fog and low-level stratus. *J. Atmos. Sci.,* **35,** 301–316.

Paluch, I. R., and D. H. Lenschow, 1991: Stratiform cloud formation in the marine boundary layer. *J. Atmos. Sci.,* **48,** 2141–2158.

Pielke, R. A., W. R. Cotton, R. L. Walko, C. J. Tremback, W. A. Lyons, L. D. Grasso, M. E. Nicholls, M. D. Moran, D. A. Wesley, T. J. Lee, and J. H. Copeland, 1992: A comprehensive meteorological modeling system—RAMS. *Meteor. Atmos. Phys.,* **49,** 69–91.

Pincus, R., and M. B. Baker, 1994: Effect of precipitation on the albedo susceptibility of clouds in the marine boundary layer. *Nature,* **372,** 250–252.

Randall, D. A., 1980: Conditional instability of the first kind upside-down. *J. Atmos. Sci.,* **37,** 125–130.

Reuter, G. W., R. de Villiers, and Y. Yavin, 1988: The collection kernel for two falling cloud drops subjected to random perturbations in a turbulent air flow: A stochastic model. *J. Atmos. Sci.,* **45,** 765–773.

Roach, W. T., R. Brown, S. J. Caughey, B. A. Crease, and A. Slingo, 1982: A field study of nocturnal stratocumulus. I. Mean structure and budgets. *Quart. J. Roy. Meteor. Soc.,* **108,** 103–123.

Slingo, A., 1989: A GCM parameterization for the shortwave radiative proper ties of water clouds. *J. Atmos. Sci.,* **46,** 1419–1427.

——, S. Nicholls, and J. Schmetz, 1982: Aircraft observations of marine stratocumulus during JASIN. *Quart. J. Roy. Meteor. Soc.,* **108,** 833–856.

Stevens, B., G. Feingold, W. R. Cotton, and R. L. Walko, 1996: Elements of the microphysical structure of numerically simulated nonprecipitating stratocumulus. *J. Atmos. Sci.* **53,** 980–1006.

Telford, J. W., and P. B. Wagner, 1981: Observations of condensation growth determined by entity type mixing. *Pure Appl. Geophys.,* **119,** 934–965.

Twomey, S., 1959: The nuclei of natural cloud formation, Part II: The supersaturation in natural clouds and the variation of cloud droplet concentration. *Geofis. Pura Appl.,* **43,** 243–249.

Tzivion, S., G. Feingold, and Z. Levin, 1987: An efficient numerical solution to the stochastic collection equation. *J. Atmos. Sci.,* **44,** 3139–3149.

——, ——, and ——, 1989: The evolution of raindrop spectra. Part II: Collisional collection–breakup and evaporation in a rainshaft. *J. Atmos. Sci.,* **46,** 3312–3327.